Canonical Profiles in Tokamaks

Yu.N. Dnestrovskij, A.Yu. Dnestrovskij, S.E. Lysenko, S.V. Cherkasov

Nuclear Fusion Institute, RRC 'Kurchatov Insitiute', Moscow, Russia

e-mail contact with main author: dnyn@nfi.kiae.ru

Abstract: The problem of the canonical profiles for a tokamak plasma with arbitrary cross-section is considered, using the principle of the free plasma energy minimum with conservation of total current, and the principle of profile consistency. The corresponding critical temperature gradients are found. The developed transport model is validated by comparison with discharges from various tokamaks. The scalings for relative temperature gradients are proposed.

1. Introduction

B.B. Kadomtsev [1] and other authors [2, 3] in 1986 analyzed the problem of relaxed states in tokamaks. To describe this state, two principles were used in [1-4]: 1) the principle of the free plasma energy minimum with the constraint of total current conservation and 2) the profile consistency principle. This problem was considered in a circular plasma cylinder and its solution was called the canonical profile. In the present work we solve the problem of the canonical profiles for a tokamak plasma with arbitrary cross-section, using the two aforementioned principles. We deduce the Euler differential equation for the canonical profile of the $\mu(\rho) = 1/q(\rho)$ function and discuss the possible boundary conditions. Then, using the canonical profile of the current density $j_c(\rho)$, we calculate the critical gradients for the temperature and create the transport model for the electron and ion temperatures and density. The model is validated by comparison with discharges from various tokamaks.

2. Canonical profile for a tokamak with arbitrary aspect ratio and cross-section shape

The free energy functional with the constraint of total current conservation can be written as:

$$F = \int_V (B_{pol}^2 / 8\pi + p/(\gamma - 1)) d^3x + \lambda_1 \int_S j\, dS\,, \qquad (1)$$

where B_{pol} is the poloidal magnetic field, p is the plasma pressure and λ_1 is a Lagrange multiplier to be defined by the boundary conditions. The self-consistency principle allows us to reduce the problem (1) to a one-dimensional one. Assuming that the profile consistency conditions are valid in the toroidal plasma, we can write

$$p=p(\mu), \quad j=j(\mu), \quad j(\mu)=\gamma\, p(\mu), \quad \mu=1/q \qquad (2)$$

where $\gamma = \text{const}(\rho)$. The minimization of F taking account of (2) leads to the Euler equation:

$$\rho^2 G\, \partial\mu_c^2/\partial\rho + (\lambda/2)\, \partial/\partial\rho\, ((1/V')\, \partial/\partial\rho(V' G \rho\mu_c)) = C\, \rho\mu_c'/V'. \qquad (3)$$

Here V' and $G=R^2\langle(\nabla\rho)^2/r^2\rangle$ are the metric coefficients, which can be found from the solution of the equilibrium problem, V is the plasma volume, prime $'$ means the derivative with respect to ρ, the multipliers C and λ are defined by the boundary conditions, and subscript "c" corresponds to the canonical profile. The boundary conditions for the circular cylinder were discussed by Kadomtsev [1]. They describe the situation when the real physical boundary conditions do not influence the processes in the plasma core. We put the boundary conditions for the toroidal plasma as follows [5]

$$\mu_c(0) = \mu(0), \quad \mu_c'(0) = 0, \quad \mu_c(a) = \mu(a), \quad X_c = X^K = \mu(a)/\mu(0), \qquad (4)$$

where μ(ρ) is the solution of the transport problem, $X_c \equiv i_c(a)/(2G_a\mu_c(a))$ is the impedance of the first order, X^K is the impedance for the Kadomtsev case, $i_c=(\mu_{00}R/B_0)\cdot j_c$ is the dimensionless current density. In order to create the transport model, we have to find the canonical profiles for the electron temperature $T_c(\rho)$ and density $n_c(\rho)$. We assume that in the relaxed quasi-steady state, the profiles of the current and the electron temperature should be close to the canonical profiles, and, hence, the canonical profiles $j_c(\rho)$ and $T_c(\rho)$ should be linked approximately by Ohm's law: $j_c(\rho) \sim T_c^{2/3}$. From this, using (2), we obtain:

$$T_c \sim j_c^{2/3}, \qquad n_c \sim T_c^{1/2} \sim j_c^{1/3} \tag{5}$$

The dimensionless critical gradients for the temperature and density can be defined using (5):

$$\Omega_{Tc} \equiv R/L_{Te} \equiv -R\, T_c'/T_c = -2/3\, R\, j_c'/j_c, \quad \Omega_{nc} \equiv -R\, n_c'/n_c = -{}^1/_3\, R\, j_c'/j_c, \tag{6}$$

Calculations show that the canonical profiles become flatter with lowering of the aspect ratio A (*FIG.* 1) or with increasing of the elongation k. A similar tendency for the experimental profiles of the electron temperature was mentioned in our previous works [6-8]. The procedure of canonical profiles calculation is described in more details in [9].

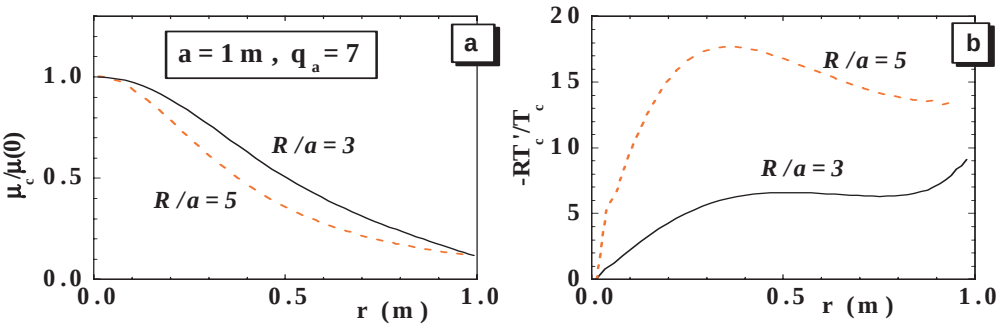

FIG. 1. Canonical profiles of $\mu_c/\mu(0)$ (a) and critical gradients $-RT_c'/T_c$ (b) for large, R/a=5, and moderate, R/a=3, aspect ratios.

3. Canonical profile transport model (CPTM)

The set of transport equations consists of the equations for the electron and ion temperatures and for the poloidal magnetic field. For simplicity we omit the equation for the plasma density. The equilibrium is obtained by the solution of the Grad-Shafranov equation. The canonical profiles are obtained by the solution of Eq. (1) with soft boundary conditions (2). The general flow chart of the CPTM is shown in *FIG.* 2.

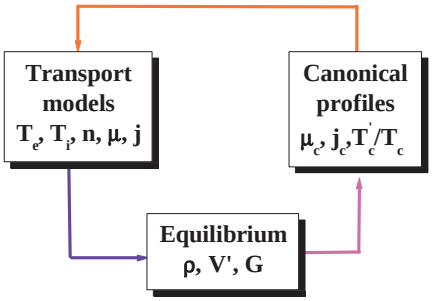

FIG. 2. Flow chart of the canonical profile transport model.

We put $\Omega_{Tci} = \Omega_{Tce} = \Omega_{Tc}$ and assume the following form of the heat fluxes for the L-mode:

$$Q_k = Q_k^{an} + Q_k^{PC} \quad (k = i, e) \tag{7}$$

$$Q_k^{an} = -\kappa_k^{an} \frac{\partial T_k}{\partial \rho}, \quad \kappa_k^{an} = n\chi_k^{an}, \quad Q_k^{PC} = \kappa_k^{PC}\ (T_k / R)(\Omega_{Tk} - \Omega_{Tc})\, H(\Omega_{Tk} - \Omega_{Tc}) \tag{8}$$

Here $H(x)$ is the Heaviside step function: $H(x)=1$, if $x \geq 0$, $H(x)=0$, if $x<0$, $\Omega_{Tk} = -R\, T_k'/T_k$ is the

relative temperature gradient. We choose the following transport coefficients [6-8]:

$$\kappa_k^{PC} = \alpha_k^{PC}\ (1/M)(a/R)^{0.75}\, q(a/2) q_{cyl}(a) (T_k(a/4))^{0.5}\, \bar{n}\, (3/R)^{1/4}/B_t = \text{const}(\rho) \qquad (9)$$

$$\chi_e^{an} = \text{const}(\rho) = \tilde{\alpha}_e \frac{(T_e(a/2))^{1/2}}{n(a/2)R} \qquad \chi_i^{an} = \chi_i^{neo} \qquad q_{cyl} = \frac{5a^2 B_t}{I_p R} \qquad (10)$$

α_e^{PC}=3.5, α_i^{PC}=5, $\tilde{\alpha}_e \approx 2$. Here M is the relative mass of the main ions, k is the elongation, T [keV], B_t [T], a and R [m], n [10^{19} m^{-3}], χ [m^2 s^{-1}] and κ [10^{19} m^{-1}s^{-1}].

4. Validation of the CPTM

Here we analyze only the electron temperature profiles, and do not consider the ion data. At first we compare the calculated T_e and experimental T_e^{exp} electron temperature profiles. In parallel we compare the calculated and experimental relative electron temperature gradients $\Omega_{Te} = -RT_e'/T_e$ and $\Omega_{Te}^{exp} = -RT_e^{exp\,\prime}/T_e^{exp}$, and show also the critical gradient $\Omega_{Tc} = -RT_c'/T_c$. We have chosen 11 DIII-D and JET shots contained in the ITER Data Base, the published data for 7 ASDEX-U shots with off-axis ECRH [10-12], 3 shots from MAST and 2 shots from T-10. We try to choose only the OH and L-mode shots, but apparently some of the DIII-D, JET, and all MAST shots, are related to the H-mode. For all chosen shots we carried out the modeling with the modified CPTM using the ASTRA code. Two types of metrics, which characterized the deviation of calculated data from experimental ones, were used:

$$dt2 = \sum_{0.2a}^{a} \left| T_e - T_e^{exp} \right| / \sum_{0.2a}^{a} T_e^{exp} \qquad (11)$$

$$dtn2 = \sum_{0.2a}^{a} \left| T_e / T_e(0.2a) - T_e^{exp} / T_e^{exp}(0.2a) \right| \Big/ \sum_{0.2a}^{a} T_e^{exp} / T_e^{exp}(0.2a) \qquad (12)$$

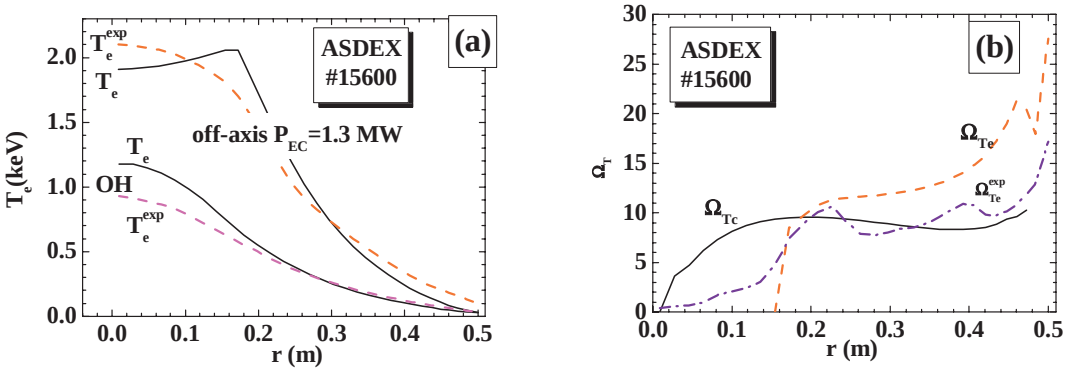

FIG. 3. Profiles of the temperature (a),and the relative and critical gradients (b) in ASDEX-U.

.

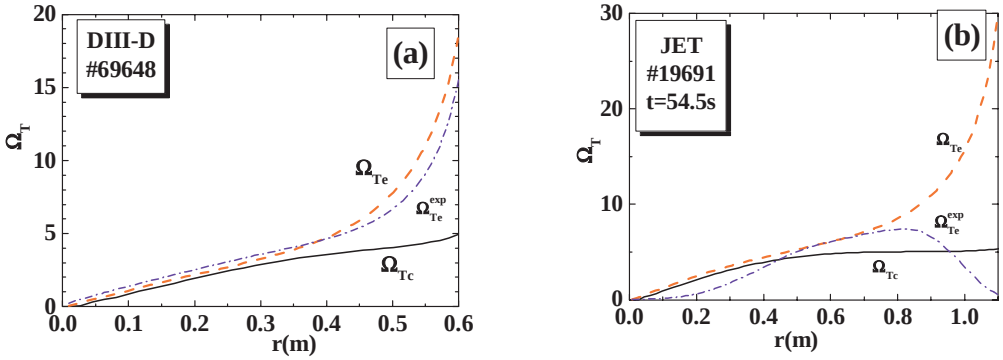

FIG. 4. Profiles of the relative and critical gradients in DIII-D (a) and JET (b).

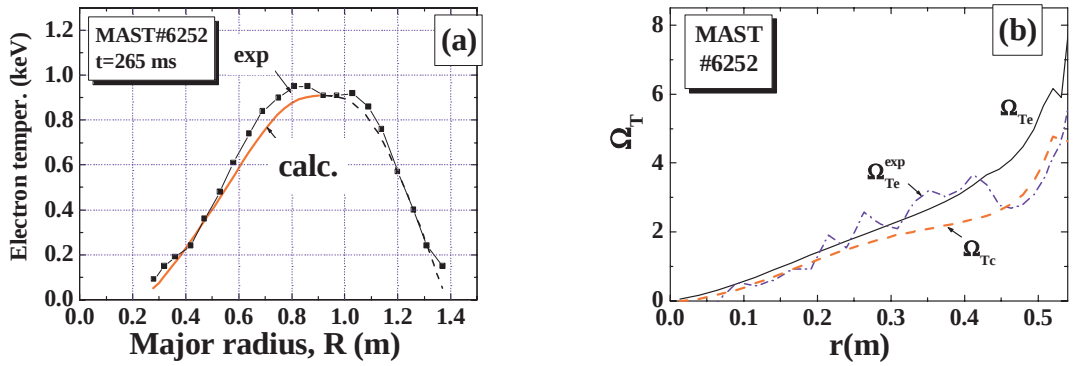

FIG. 5. Profiles of the temperature (a), and the relative and critical gradients (b) in MAST.

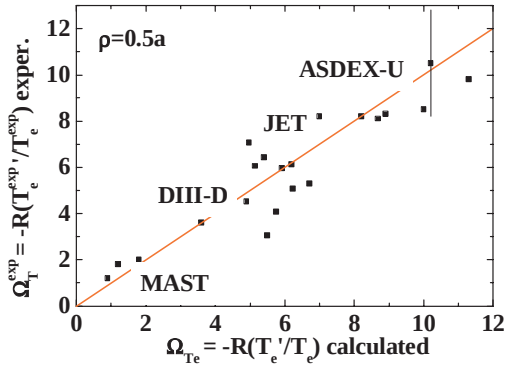

FIG. 6. Comparison of experimental and calculated relative gradients.

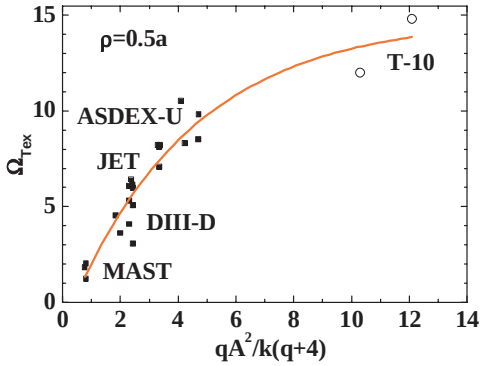

FIG. 7. Experimental relative gradient vs. scaling parameter $qA^2/k(q+4)$.

As we noted before, modification of the CPTM consists of the change of the Kadomtsev canonical profile $\mu_c^K(\rho)$ to the solution of Eq. (3) for $\mu_c(\rho)$. In *FIGS* 3-5 we compare the calculations and experimental results for ASDEX-U, DIII-D, JET and MAST. The quality of our simulation for T_e profiles is shown in *FIGS* 3a and 5a. The relative gradients $\Omega_{Te}= -RT_e'/T_e$, $\Omega_{Te}^{exp} =-RT_e^{exp}{}'/T_e^{exp}$ and critical gradients $\Omega_{Tc}=-RT_c'/T_c$ for all four devices are shown in *FIGS* 3b, 4, and 5b. It is seen that these profiles are flat in the gradient zone; therefore we can characterize them by magnitudes in the mid-radius. A comparison of calculated and experimental values of Ω_{Te} and Ω_{Te}^{exp} is provided in *FIG*. 6. The error bar for one of the ASDEX-U shots is also shown. We see that the experimental and calculated relative gradients reasonably correspond to each other.

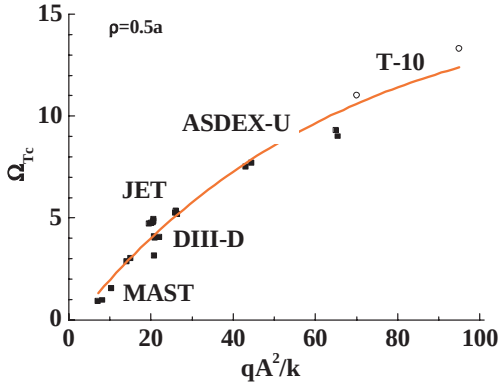

FIG. 8. Calculated critical gradient vs. scaling parameter qA^2/k.

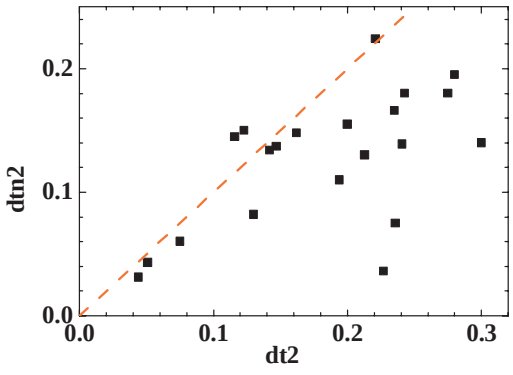

FIG. 9. Normalized deviation of T_e from T_e^{exp} vs. their linear deviation.

The calculations show that the peakedness of the canonical profile increases if either the aspect ratio $A=R/a$, or the q value rises. This peakedness also increases if the elongation k diminishes. So the parameter qA^2/k could be the scaling parameter for the relative gradients. The power 2 for the aspect ratio is the consequence of the normalization by the major radius in the dimensionless relative gradients. If we take into account the asymptote of the critical gradient Ω_c in the Kadomtsev case ($R\to\infty$), $\Omega_c={}^{16}/_{3}\cdot Aq/(q+4)$, then the scaling parameter can be modified to $qA^2/(k(q+4))$. In is unclear *a priori* which parameter is better, so we test them both. The experimental values of $\Omega_{T_e}^{\exp}$ versus the scaling parameter $qA^2/(k(q+4))$ are shown in *FIG*. 7. Two points for the T-10 tokamak with circular plasma cross-section and large aspect ratio A=5 are also shown. It is seen that all points are positioned in the vicinity of some curve with decreasing slope. *FIGURE* 8 shows the dependence of the calculated critical gradient Ω_c on the parameter qA^2/k. We see that in this case the scattering of points is also not large. So now it is impossible to make a final choice concerning the scaling parameter for relative gradients. *FIGURE* 9 shows the quality of simulation by the CPTM. We see that the linear deviations (11) are twice as large as the normalized deviations (12). This means that this model describes the gradients better than the absolute temperatures values.

5. Conclusion

The modified CPTM was validated using experimental data from several tokamaks. The modification is based on a more general approach, which allows us to find the canonical profile $\mu_c(\rho)$ for tokamak plasmas with arbitrary cross-sections and aspect ratios. The critical temperature gradient $\Omega_c=R/L_{Tc}$, which could be included into the heat fluxes, can be expressed through the obtained canonical profile. Modeling of the chosen set of shots has shown a good correlation between the experimental and calculated electron temperature profiles. Analysis of the experimental and calculated relative temperature gradients $\Omega_{Te}= -RT_e'/T_e$ allows us to find the possible scaling variables (qA^2/k, $qA^2/k(q+4)$), which can determine the absolute values of Ω_{Te}. This fact allows one to explain the visible contradictions in the interpretation of the experimental data from DIII-D and several European tokamaks [10-12].

This work was supported by Grant RFBR 00-15-96536, Minatom RF and the UKAEA Agreement QS06588.

References

[1] KADOMTSEV, B.B., Sov. J. Plasma Phys. **13** (1987) 443.
[2] BISKAMP, D., Comments Plasma Phys. Control. Fusion **10** (1986) 165.
[3] HSU, J.Y., CHU, M.S., Phys. Fluids **30** (1987) 1221.
[4] KADOMTSEV, B.B., Plasma Phys. Control. Fusion **34** (1992) 1931.
[5] DNESTROVSKIJ, Yu.N., et al., Nucl. Fusion **38** (1998) 373.
[6] DNESTROVSKIJ, Yu.N., PEREVERZEV, G.V., Plasma Phys. Control. Fusion **30** (1988) 47.
[7] DNESTROVSKIJ, Yu.N., et al., Nucl. Fusion **31** (1991) 1877.
[8] DNESTROVSKIJ, Yu.N., et al., Plasma Phys. Repts **26** (2000) 539.
[9] DNESTROVSKIJ, Yu.N., et al., Plasma Phys. Repts **28** (2002) 963.
[10] RYTER, F., et al., Plasma Phys. Control. Fusion **43** (2001) A323.
[11] RYTER, F., et al., Control. Fusion Plasma Phys. (Proc. 29th EPS Conf. Montreux, 2002) paper P-1.048, ECA, V. 26B (2002).
[12] LEUTERER, F., et al., ECE and ECRH (Proc. 12th Int. Workshop, Aix-en-Provence, France, 2002), http://wshop.free.fr/ec12/.